

DFT Study of an Inner-Sphere Mechanism in the Hydrogen Transfer from a Hydroxycyclopentadienyl Ruthenium Hydride to Imines

Timofei Privalov,^{*,†} Joseph S. M. Samec,[‡] and Jan-E. Bäckvall[‡]

Department of Chemistry, Organic Chemistry, Royal Institute of Technology (KTH), SE-100 44 Stockholm, Sweden, and Department of Organic Chemistry, Arrhenius Laboratory, Stockholm University, SE-106 91 Stockholm, Sweden

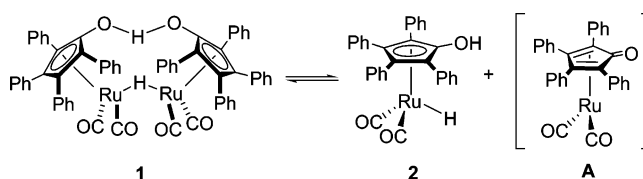
Received February 23, 2007

A combination of the DFT method with the computational description of environmental effects by solvent was applied to a theoretical study of the hydrogen transfer to imines by [2,3,4,5-Ph₄(η^5 -C₄COH)-Ru(CO)₂H] (**2**) within a molecular model that closely mimics the authentic reaction conditions. A consistent polarizable continuum solvent model (PCM) was instrumental and necessary in achieving stability of the computational model. Environmental effects by solvent were also considered in an extended model with an addition of explicit solvent molecules within the PCM. The study elucidates an inner-sphere mechanism in detail. Intermediate complexes and transition states are characterized. Three distinct energy barriers along the reaction coordinate are predicted when solvent effects are taken into account. The imine coordinates to ruthenium via ring slippage with an energy barrier of about 15 kcal/mol. Close in energy (12 kcal/mol) is the transition state of the hydride transfer, which gives an (η^2 -cyclopentadienone)-ruthenium amine intermediate. The presence of Ph groups on the Cp ring facilitates the ring slippage that occurs on imine coordination. This η^2 -intermediate finally rearranges to the corresponding (η^4 -cyclopentadienone)ruthenium amine complex via a transition state at 9 kcal/mol. The stable ruthenium amine complex was verified against an X-ray structure of the corresponding complex. Inclusion of the solvent (by PCM or explicit molecules) was required to stabilize low-hapticity intermediates and transition state structures.

Introduction

Transition metal-catalyzed hydrogen transfer has attracted considerable attention during the past 10–15 years.^{1,2} A variety of new catalysts have been reported that are highly efficient for transferring hydrogen from a hydrogen donor (e.g., an alcohol) to a hydrogen acceptor (e.g., a ketone). Catalytic hydrogen transfer reactions have been successfully applied to selective organic transformations including enantioselective reactions.^{1e,3} In 1985 Shvo reported on the dimeric catalyst **1**, which breaks up into the monomers **2** and **A** (Scheme 1).^{4,5} The former monomer (**2**) is able to hydrogenate a hydrogen acceptor, whereas the latter monomer (**A**) can dehydrogenate a hydrogen donor. These processes interconvert **2** and **A**. Complex

Scheme 1. Dimeric Precatalyst **1** in Equilibrium with Active Monomers **2** and **A**



1 has been shown to be an active catalyst in hydrogen transfer reactions involving alcohols and ketones (aldehydes).^{1a,b,d,6–8} Notably, the catalyst has shown high stability, and this has been advantageous in aerobic oxidations of alcohols and also in the dynamic kinetic resolution of secondary alcohols.^{7,8} We have previously reported that **1** can be successfully used as a catalyst

* Corresponding author. E-mail: priti@kth.se.

[†] Royal Institute of Technology.

[‡] Stockholm University.

(1) (a) Gladiali, S.; Mestroni, G. In *Transition Metals in Organic Synthesis*; Beller, M., Bolm, C., Eds.; Wiley-VCH: Weinheim, 1998; Vol. 2, p 97. (b) Bäckvall, J.-E.; Chowdhury, R. L.; Karlsson, U.; Wang, G.-Z. In *Perspectives in Coordination Chemistry*; Williams, A. F., Floriani, C., Merbach, A. E., Eds.; Verlag Helvetica Chimica Acta: Basel, 1992; p 463. (c) Abdur-Rashid, K.; Clapham, S. E.; Hadzovic, A.; Harvey, J. N.; Lough, A. J.; Morris, R. H. *J. Am. Chem. Soc.* **2002**, *124*, 15104. (d) Samec, J. S. M.; Bäckvall, J. E.; Andersson, P. G.; Brandt, P. *Chem. Soc. Rev.* **2006**, *35*, 237–248. (e) Gladiali S.; Alberico, E. *Chem. Soc. Rev.* **2006**, *35*, 226–236.

(2) (a) Budzelaar, P. H. M.; Engelberts, J. J.; van Lenthe, J. H. *Organometallics* **2003**, *22*, 1562–1576. (b) Fan, H.-J.; Hall, M. B. *Organometallics* **2001**, *20*, 5724–5730.

(3) Noyori, R.; Hashiguchi S. *Acc. Chem. Res.* **1997**, *30*, 97.

(4) Blum, Y.; Czarkie, D.; Rahamim, Y.; Shvo, Y. *Organometallics* **1985**, *4*, 1459.

(5) Karvembu, R.; Prabhakaran, R.; Natarajan, K. *Coord. Chem. Rev.* **2005**, *249*, 911–918.

(6) (a) Shvo, Y.; Czarkie, D.; Rahamim, Y. *J. Am. Chem. Soc.* **1986**, *108*, 7400. (b) Menashe, N.; Shvo, Y. *Organometallics* **1991**, *10*, 3885.

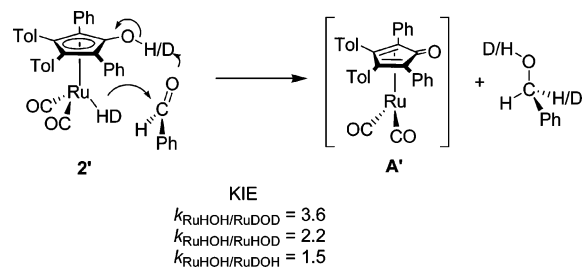
(7) (a) Csajernyik, G.; Ell, A. H.; Fadini, L.; Pugin, B.; Bäckvall, J.-E. *J. Org. Chem.* **2002**, *67*, 1657. (b) Wang, G.-Z.; Andreasson, U.; Bäckvall, J.-E. *J. Chem. Soc., Chem. Commun.* **1994**, 1037.

(8) (a) Larsson, A. L. E.; Persson, B. A.; Bäckvall, J.-E. *Angew. Chem., Int. Ed. Engl.* **1997**, *36*, 1211. (b) Persson, B. A.; Larsson, A. L. E.; Ray, M. L.; Bäckvall, J.-E. *J. Am. Chem. Soc.* **1999**, *121*, 1645. (c) Huerta, F. F.; Minidis, A.; Bäckvall, J.-E. *Chem. Soc. Rev.* **2001**, *30*, 321. (d) Pàmies, O.; Bäckvall, J.-E. *Chem. Rev.* **2003**, *8*, 3247.

(9) (a) Samec, J. S. M.; Bäckvall, J.-E. *Chem.—Eur. J.* **2002**, *13*, 2955. (b) Samec, J. S. M.; Mony, L.; Bäckvall, J.-E. *Can. J. Chem.* **2005**, *83*, 909.

(10) (a) Ell, A. H.; Samec, J. S. M.; Brasse, C.; Bäckvall, J.-E. *Chem. Commun.* **2002**, *10*, 1144. (b) Ell, A. H.; Johnson, J. B.; Bäckvall, J.-E. *Chem. Commun.* **2003**, *14*, 1652. (c) Samec, J. S. M.; Ell, A. H.; Bäckvall, J.-E. *Chem.—Eur. J.* **2005**, *11*, 2327. (d) Ibrahim, I.; Samec, J. S. M.; Bäckvall, J.-E.; Córdova, A. *Tetrahedron Lett.* **2005**, *46*, 3965.

Scheme 2. Hydrogenation of Benzaldehydes by 2' and Proposed Concerted Outer-Sphere Mechanism

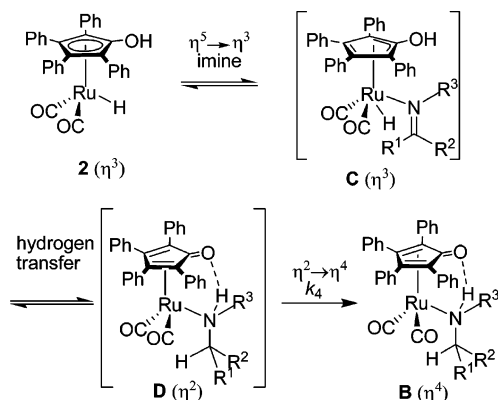


in the reduction of imines,⁹ the oxidation of amines,¹⁰ and the racemization of amines,¹¹ via hydrogen transfer. The latter reaction was recently successfully applied to the dynamic kinetic resolution of amines.¹²

There has been a recent interest in the mechanism of catalyst **1** concerning its reaction with different substrates.^{10b,13–16} On the basis of kinetic deuterium isotope effects it has been proposed that the mechanism involving alcohols and ketones (aldehydes) involves a concerted rate-determining hydrogen transfer.^{14,15} In this proposed mechanism the hydride and the acidic proton of **2** (**2'**) are transferred in a concerted manner to the carbonyl outside the coordination sphere of the metal (Scheme 2).¹⁴

On the other hand, the mechanism involving amines and imines shows clear differences from that of ketones (aldehydes).^{10b,13,16} While electron-deficient imines behave like alcohols and ketones (aldehydes) in their reaction with **2** and proceed via a concerted rate-determining hydrogen transfer, electron-rich imines do not.^{13,16} Furthermore, dehydrogenation of amines by **A** was shown to occur via a stepwise mechanism.^{10b} Two different mechanisms have been proposed for the hydrogen transfer of imines by **2**. One of the mechanisms involves an outer-sphere pathway in which the imine is not coordinated to ruthenium.^{14a,16} In the other mechanism an inner-sphere pathway was proposed with coordination of the imine to ruthenium in an η^3 -Cp intermediate.¹³ Casey has previously provided experimental support for the outer-sphere mechanism,¹⁶ including some computational evaluation of that mechanism. Recently, we have obtained new experimental results that support the inner-sphere pathway.^{13b} However, a comprehensive computational investigation of an inner-sphere pathway has not yet been published. In the present article the density functional theory (DFT) was applied to study the hydrogen transfer reaction from active species **2** of catalyst **1** to imines via an inner-sphere reaction pathway. The objective of the present study is not to eliminate one mechanism from another solely on the basis of computational data, but to describe an inner-sphere mechanism within a framework of a realistic and accurate molecular model. Thus, the prime objective of this computational study has been to examine an inner-sphere reaction mode in which the imine coordinates to ruthenium followed by insertion of the imine into

Scheme 3. Proposed Inner-Sphere Mechanism for Imines by 2



the Ru–H bond (Scheme 3) and to determine factors that are important for accurate calculation of activation energies associated with rate-limiting steps. Recent theoretical studies,^{17,18} demonstrating that intimate details of complex reaction mechanisms can be treated well with computational methods, encouraged us to theoretically study the hydrogen transfer from **2** to imines.

The coordination of a substrate to the metal, required by the proposed inner-sphere reaction mechanism, is possible only if there is an empty coordination site on the metal and the electronic configuration of the metal is such that it can contribute to the bonding orbital in a metal–ligand pair. This strongly suggests that a $\eta^5 \rightarrow \eta^3$ ring slip of the Cp ligand must occur on coordination of the imine. Haptotropic shifts in organometallic fragments, such as $\text{Ru}(\text{CO})_2$ and $\text{Mn}(\text{CO})_3$, within one ring or even between two rings of a heterocyclic complex are relevant for the mechanism of associative substitution/addition reactions when a vacant coordination site on the metal is required.¹⁹ Lower hapticity intermediates are quite difficult to isolate, something that increases the value of computational modeling.

While most chemistry occurs in solution, computational chemistry is usually concerned with isolated molecules.^{20,21} Due to prolonged calculation times, it is tempting to perform calculations in the gas phase, use low basis sets, and abstract groups of molecule that are not directly reacting. However, the situation is rapidly changing, as new hardware and new implementations of algorithms have appeared for treating the quantum-mechanical electronic structure of large molecular systems surrounded by solvent.²²

Results and Discussion

Geometry optimizations of all intermediate complexes and transition states were carried out using the B3LYP functional²³

(17) (a) P. E. M.; Blomberg, M. R. A. *Chem. Rev.* **2000**, *100*, 421–437. (b) Noodelman, L.; Lovell, T.; Han, W.-G.; Li, J.; Himo, F. *Chem. Rev.* **2004**, *104*, 459. (c) Friesner, R. A.; Guallar, V. *Annu. Rev. Phys. Chem.* **2005**, *56*, 389.

(18) (a) Paavola, S.; Zetterberg, K.; Privalov, T.; Csöregy, I.; Moberg, C.; *Adv. Synth. Catal.* **2004**, *346*, 237. (b) Privalov, T.; Linde, C.; Zetterberg, Z.; Moberg, C. *Organometallics* **2004**, *24*, 885. (c) Schultz, M.; Adler, R.; Zierkiewicz, W.; Privalov, T.; Sigman, M. *J. Am. Chem. Soc.* **2005**, *127*, 8499. (d) Zierkiewicz, W.; Privalov, T. *Organometallics* **2005**, *24*, 6019–6028.

(19) Veiros, L. F. *Organometallics*, **2000**, *19*, 5549, and references therein.

(20) Reichardt, C. *Solvents and Solvent Effects in Organic Chemistry*, 3rd ed.; Wiley: New York, 2003; ISBN 3-527-30618-8.

(21) *Computational Chemistry: Reviews of Current Trends*; Leszczynski, J., Ed.; ISSN 1793-0979. A great deal of computational technical details and background references could be found in a databank provided by Schrödinger, Inc., Portland, OR, and Gaussian Inc.; see also refs 4 and 5.

(11) Pàmies, O.; Ell, A. H.; Samec, J. S. M.; Hermanns, N.; Bäckvall, J.-E. *Tetrahedron Lett.* **2002**, *26*, 4699.

(12) Paetzold, J.; Bäckvall, J.-E. *J. Am. Chem. Soc.* **2005**, *127*, 17620.

(13) (a) Samec, J. S. M.; Ell, A. H.; Bäckvall, J.-E. *Chem. Commun.* **2004**, 2748. (b) Samec, J. S. M.; Ell, A. H.; Åberg, J. B.; Privalov, T.; Eriksson, L. Bäckvall, J.-E. *J. Am. Chem. Soc.* **2006**, *128*, 14293.

(14) (a) Casey, C. P.; Singer, S. W.; Powell, D. R.; Hayashi, R. K.; Kavana, M. *J. Am. Chem. Soc.* **2001**, *123*, 1090. (b) Casey, C. P.; Johnson, J. B. *Can. J. Chem.* **2005**, *83*, 1339.

(15) Johnson, J. B.; Bäckvall, J.-E. *J. Org. Chem.* **2003**, *68*, 7681.

(16) (a) Casey, C. P.; Johnson, J. B. *J. Am. Chem. Soc.* **2005**, *127*, 1883. (b) Casey, C. P.; Bikzhanova, G. A.; Cui, Q.; Guzei, I. A. *J. Am. Chem. Soc.* **2005**, *127*, 14062.

with the lacvp*/6-31G(d) basis set.^{24,25} All degrees of freedom were optimized, while transition states were obtained by utilizing a QST-guided search. Additionally, B3LYP energies were evaluated for the optimized geometry using a larger triple- ζ basis, lacv3p*/6-311+G(d), with additional diffuse and polarization functions. The solvent, including geometry optimization in the solvent reaction field, was modeled using the polarized medium (PCM) with additional solvent molecules and/or water molecules in the second coordination sphere of the complexes studied. All explicit solvent conformations were optimized within a standard and accurate geometry optimization algorithm, as implemented in Jaguar 6.0, which also results in an accurate description of solvent–solvent interactions. Employment of the PCM together with explicit solvent typically results in considerable increase of the accuracy by way of better accounting for solvent–solvent interaction and for boundary effects in a molecular model of a limited size. See more in Technical Details.

Solvent and Substituent Effects. Previous gas phase calculations carried out for the hydrogenation of imines by the tetrahydro analogue of **2** favored a concerted outer-sphere mechanism (cf. Scheme 2).^{16b} However, it has been experimentally observed that there is a significant solvent effect in the reductions by **2**.^{9a,14} For example, it was found that water improves the catalytic transfer hydrogenation^{9a} of imines and the stoichiometric hydrogenation¹⁴ of benzaldehyde by **2**; the results from the reactions performed under dry conditions were found to be unreliable and difficult to reproduce. We therefore argued that the role of the solvent is of importance for the optimization of the energies of transition states and intermediates along the reaction coordinate. The PCM within a combined hybrid model with a number of explicit solvent molecules may be considered, as it has previously been shown to be successful when studying other complex reaction systems.²⁶

One example of such an extended model, which has also been applied to all considered complexes, is shown in Figure S1 (Supporting Information), which demonstrates not only that the η^3 ring-slipped Ru–Cp structure could well be stabilized by an interaction with solvent molecules within the continuum solvent model, but that it may also benefit from an interaction with the carbon atom on the neighboring phenyl ring. The Cp ring offers several possible coordination modes with several nonequivalent positions for the η^2 and η^3 coordinations. Therefore several η^3 and η^2 ring-slipped Ru–Cp structures were computationally evaluated. *The common denominator of all computed structures is that lower hapticity complexes are unstable in the model*

(22) The self-consistent reaction field (SCRf) method is explained in the Supporting Information. The Jaguar 6.0 package treats solvated molecular systems with the SCRf method, using its own Poisson–Boltzmann solver, which makes it possible to compute solvation energies and minimum-energy solvated structures of solvated transition states. For details see: (a) Tannor, D. J.; Marten, B.; Murphy, R.; Friesner, R. A.; Sitkoff, D.; Nicholls, A.; Ringnalda, M.; Goddard, W. A., III; Honig, B. *J. Am. Chem. Soc.* **1994**, *116*, 11875. (b) Marten, B.; Kim, K.; Cortis, C.; Friesner, R. A.; Murphy, R. B.; Ringnalda, M. N.; Sitkoff, D.; Honig, B. *J. Phys. Chem.* **1996**, *100*, 11775. (c) Cramer, C. J.; Truhlar, D. G. *Chem. Rev.* **1999**, *99*, 2161–2200.

(23) (a) Becke, A. D. *J. Chem. Phys.* **1993**, *98*, 5648. (b) Lee, C.; Yang, W.; Parr, R. G. *Phys. Rev. B* **1988**, *37*, 785.

(24) Hay, P. J.; Wadt, W. R. *J. Chem. Phys.* **1985**, *82*, 299.

(25) (a) Hehre, W. J.; Ditchfield, R.; Pople, J. A. *J. Chem. Phys.* **1972**, *56*, 2257. (b) Francl, M. M.; Pietro, W. J.; Hehre, W. J.; Binkley, J. S.; Gordon, M. S.; Defrees, D. J.; Pople, J. A. *J. Chem. Phys.* **1982**, *77*, 3654. (c) Hariharan, P. C.; Pople, J. A. *Theor. Chim. Acta* **1973**, *28*, 213.

(26) (a) Cimino, P.; Barone, V. *THEOCHEM* **2005**, *729*, 1–9. (b) Amovilli, C.; Barone, V.; Commi, R.; Cancès, E.; Cossi, M.; Mennucci, B.; Pomelli, C. S.; Tomasi, J. *Adv. Quantum Chem.* **1999**, *32*, 227. See also: Brancato, G.; Di Nola, A.; Barone, V.; Amadei, A. *J. Chem. Phys.* **2005**, *122* (15), 154109/1–154109/9.

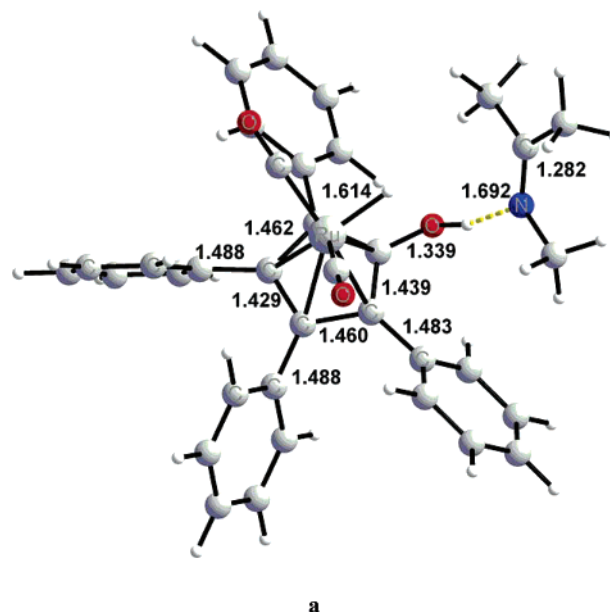


Figure 1. B3LYP/lacvp*-optimized η^5 -Ru–H complex (**2**) with the weakly bonded imine in the outer coordination sphere. Ru–C distances are 2.402, 2.329, 2.312, 2.328, and 2.349 Å with respect to the C atoms on the Cp ring (clockwise, starting from the carbon to the C of the COH group). OH bond length is 1.021 Å. All distances are in Å.

*without continuum solvent, and eventually they collapse to the coordinatively saturated η^5 Ru–Cp structure.*²⁷ However, solvent effects (PCM or/and an addition of a small amount of explicit solvent molecules) allow for reliable and reproducible stabilization of lower hapticity Ru–Cp structures. Gas phase calculations for the hydrogenation of imines by a tetrahydro analogue of **2** were carried out earlier in the framework of an outer-sphere mechanism; solvent effects were estimated by single-point calculations at the gas-phase-optimized geometries with implicit solvent model.^{16b}

Ru–Imine Complexes (formation of a). The starting point in our computational study of the reaction mechanism is the adduct of model imine²⁸ Me–N=C(Me)₂ with **2** (**a**, Figure 1). There are several mechanistically important details about adduct **a**. First, this adduct is formed via an OH–N hydrogen bond, which is quite flexible and where the electronic binding energy is –12 and –9.6 kcal/mol in the gas phase and solvent, respectively. Larger substrates, with electron-deficient groups, e.g., *N*-phenyl-(1-phenylethylidene)amine, have a somewhat smaller binding energy of about –6 to –5 kcal/mol (the corresponding energy difference is comparable to the error of an accurate DFT method, which is about 2 to 5 kcal/mol). Second, the substrate competes against solvent molecules and other species, i.e., water, for this binding site. Therefore, a correct description of the binding and an appropriate calculation of the binding energy require the presence of solvent molecules in the first and also partially in the second coordination spheres of the binding site. Third, the orientation of the RuH(CO)₂ unit is not fixed with respect to the direction of the COH of the Cp ring. There are several possible configurations of **2** with rotated

(27) Computational evaluation of lower hapticity Ru–Cp structures is complicated due to the shallow potential in the direction of the movement of the RuH(CO)₂ group perpendicular to the C–C or C–C–C ring fragment. Quasi-stable intermediates were often obtained for a quite large number of conventional energy minimization steps. These problems were essentially absent in the model with explicit solvent molecules.

(28) A series of authentic imine substrates was used in the verification study as well (see details in Supporting Information).

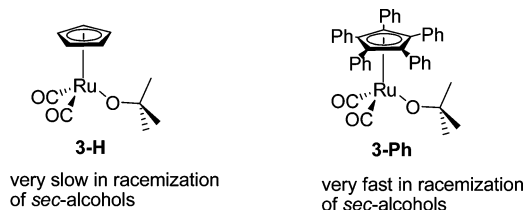


Figure 2. Phenyl groups promote ring slippage.

RuH(CO)₂ that have almost degenerate electronic energy. Importantly, the description of the interaction between the imine and the COH of the Cp ring is strongly dependent on the quality of the basis set. It was found that small basis sets, i.e., lacvp, favor protonation of the imine, which contradicts the structures that were optimized with larger basis sets, including lacvp* and larger basis sets.

Coordination via Ring Slippage (TS1). For the imine to coordinate to **2** there must be a vacant coordination site at the metal. It has previously been proven that the CO does not dissociate in the hydrogen transfer from **2** to benzaldehyde.¹⁴ The only alternative to create a vacant coordination site at the metal is therefore a ring slippage. The stability of the η^5 Ru–Cp unit makes this search tricky. It appears that the phenyl substituents play an important role in making the Ru–Cp unit more flexible. We have not found any ring slip TS in the simplified model without phenyl substituents, and this could partially explain why only a concerted outer-sphere mechanism was considered using a simplified tetrahydro analogue of **2**.^{16b} Interestingly, the phenyl groups have been proven experimentally to be very important for the related racemization catalyst **3** (Figure 2).²⁹ Since **3** does not have the ligand bifunctional outer-sphere option of catalyst **2**, racemization of alcohols by **3** via β -elimination requires the formation of a η^3 -Cp–Ru intermediate. The parent Cp analogue **3-H** is very slow in the racemization of (*S*)-1-phenylethanol. In contrast, the pentaphenyl-substituted analogue **3-Ph** is a very active complex and completely racemized the same alcohol within 10 min using only 0.5 mol % catalyst.²⁹ Also, Crabtree has reported that substituting the Cp ring with one phenyl group on an IrH species makes the catalyst behave similar to an indenyl ligand, which is known to promote ring slippage in associative mechanisms.³⁰

Whereas the TS search in the absence of the phenyl groups was unsuccessful, we were able to find a TS in the complete model with phenyl groups (Figure 3). Frequency analysis of **TS1** and relaxation of the geometry of this complex confirmed that this is indeed a transition state structure with a shallow saddle point. We have successfully performed a series of optimizations of η^3 -Cp–Ru transition states, similar to **TS1**, with the lacvp* basis set³¹ within the automatic QST-guided procedure, as implemented in the Jaguar 6.0 computational package. The set of representative structures is given in the Supporting Information. Both η^3 and η^2 transition states were found. Importantly, the η^3 -type transition state was almost 11 kcal/mol more stable than the η^2 one (this may be of no surprise since a η^3 -allyl complex is expected to be more stable than a complex via η^2 -coordination since the latter leads to formal charge separation or unpaired electrons).

The electronic activation energy of **TS1** is 23 kcal/mol in the gas phase, while solvent effects within PCM reduce the

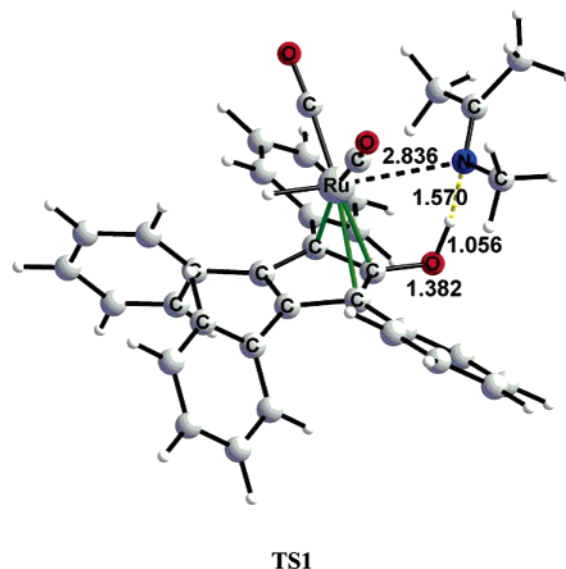


Figure 3. B3LYP/lacvp*-optimized η^3 Ru–Cp transition state with an imine in a weak coordination position with respect to both Ru and OH. Three Ru–C bonds are marked green. Ru–H distance is 1.572 Å. QST-guided search method was used. All bond distances are in Å.

energy by 8 kcal/mol to a reasonable activation energy of 15 kcal/mol. It is not surprising that the Cp ring slip requires more energy in the gas phase model. In the presence of explicit solvent molecules and/or in the continuum solvent model to represent the bulk solvent, the energy difference between properly optimized low- and high-hapticity complexes becomes smaller. The reason for the failure of a simple gas phase model is related to the increase in the Coulomb interaction between the positively charged metal, i.e., Ru(II), and the somewhat negatively charged Cp ring when the ring-slipped structures are considered. Lower hapticity complexes have a larger energy of the separated positive and negative parts, i.e., the Cp ring and the metal ion, and this interaction is not well described without solvent. This indicates that the effect of the solvent environment plays an important role and that the lower hapticity complex or transition state will “pick up” stabilization energy to a larger extent than the reference η^5 complex **a** by interacting with the solvent molecules. While the coordination of the imine to the ruthenium proceeds via the η^3 -**TS1**, the imine and the ruthenium form the rather stable intermediate **c**, which may be described as an unsymmetrical η^3 or a η^2 complex (Figure 4). Intermediate **c** is only 3 kcal higher in energy than adduct **a** when solvent effects (PCM solvent stabilization energy for **c** is 7 kcal/mol larger than that for **a**) are accounted for, while at the gas phase level of theory this transformation is endothermic by about 10 kcal/mol. Accordingly, accounting for extra solvent effects in the complete hybrid model, the energy difference between Ru–imine complex **c** and precursor **a** becomes rather small. The weaker Ru–Cp interaction in **c** is compensated by a stronger Ru–N bond.

If the coordination is the rate-determining step, an electron-rich imine that is a better nucleophile would form ruthenium amine complexes more easily than electron-deficient ones. Experimentally, a correlation was indeed found between the electronic property of the imine and the temperature at which the amine generated from the imine and hydride **2** gave a stable Ru–amine complex.^{13b,16} It was found that electron-rich imines gave Ru–amine complexes at lower temperatures than electron-deficient imines. Also in hydrogen transfer reactions involving imines and amines catalyzed by **1** a correlation between the

(29) (a) Csornyik, G.; Bogár, K.; Bäckvall, J.-E. *Tetrahedron Lett.* **2004**, 45, 6799. (b) Martín-Matute, B.; Edin, M.; Bogár, K.; Kaynak, F. B.; Bäckvall, J.-E. *J. Am. Chem. Soc.* **2005**, 127, 8817.

(30) Habib, A.; Tanke, R. S.; Holt, E. M.; Crabtree, R. H. *Organometallics* **1989**, 8, 1225.

(31) Even a small basis set like lacvp performs rather well.

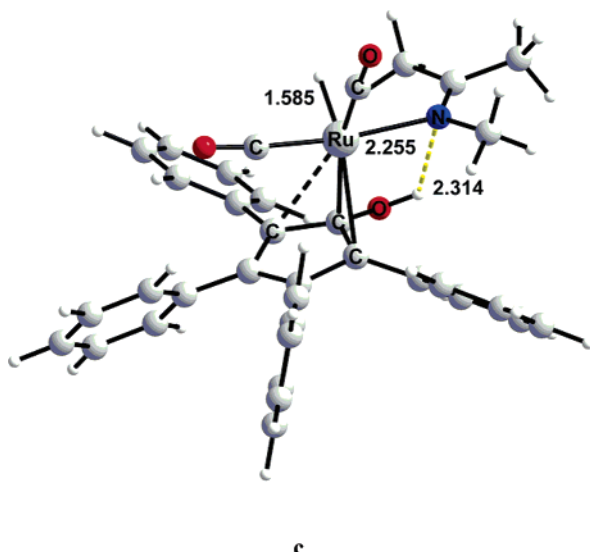


Figure 4. B3LYP/lacvp*-optimized Ru–Cp complex (unsymmetrical η^3 or η^2) with an imine coordinated to the ruthenium ion of hydroxycyclopentadienyl ruthenium hydride without additional solvent molecules. All bond lengths are in Å.

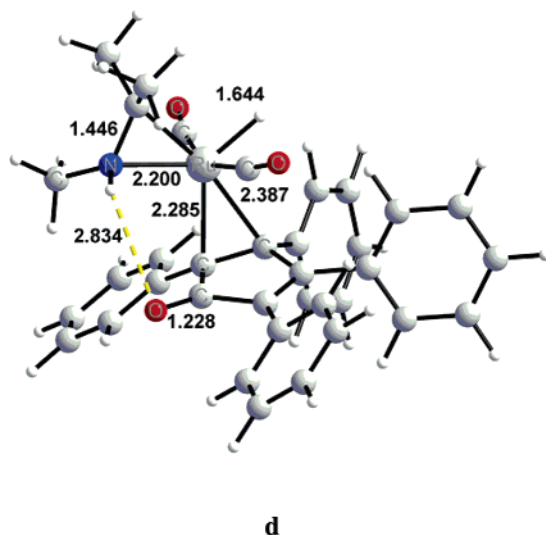


Figure 5. B3LYP/lacvp*-optimized η^2 Ru–Cp complex with the protonated imine that shows a bidentate binding motif with respect to Ru. All bonds lengths are in Å.

rate and the electronic property of the substrate was found. Thus, in all three different catalytic reactions including transfer hydrogenation, transfer dehydrogenation, and racemization via hydrogen transfer, electron-rich substrates gave higher rates than electron-deficient substrates.

Proton Transfer. After coordination the hydrogen transfer occurs. There are three different possibilities for the hydrogen transfer to occur: (i) a concerted proton and hydride transfer, (ii) proton transfer followed by hydride transfer, or (iii) hydride transfer followed by proton transfer. Our calculations suggest that the protonation of the imine is likely to occur first and to be the fast reaction step. Environmental effects in the presence of small amounts of a protic solvent tilt the energy balance further to the side of the η^2 complex **d** (Figure 5), which is the analogue of **c** but with the protonated imine and the η^2 -binding of the imines. The solvent molecule, i.e., water, is able to bridge the N atom with the OH group on the Cp ring. Such a bridge makes the proton transfer even more efficient.

It is interesting to note that when a *tight* Ru–N bond is formed between the ruthenium ion and the imine (e.g., in **d**), the η^2 metal coordination geometry is preferred over the η^3 geometry in the computed structures with or without accounting for solvent effects. (**TS1** does not have a *tight* Ru–N bond, and thus η^3 -geometry is more stable.) This is in agreement with previous studies of intramolecular rearrangements with metal–Cp systems.³² Environmental effects by solvent seem to amplify this difference with a clear preference for the more flexible η^2 metal coordination geometry. Also, and importantly, the presence of a protic admixture in the solvent eliminates the difference between Ru–imine and protonated imine–Ru complexes since the proton can easily be shuffled back and forth between the N atom and OH group when bridged by solvent and could also provide variable degrees of stabilization of the charged parts of Ru–Cp complexes.

Migratory Insertion (TS2). The search for transition states that might be responsible for the hydride transfer from ruthenium to the carbon atom of the protonated C=N moiety revealed that only η^2 -Cp-like structures could be predicted regardless of both the initial configuration and the complexity of the environmental model. We have found that also the most simplistic model with no additional solvent molecules works well in terms of the structure search, but fails completely in terms of predicting the energy of TS2. On the basis of the gas phase optimizations only, the gas phase transition state energy is 41 kcal/mol with respect to the gas phase energy of the precursor **a**. The high energy of the gas phase transition state is due to (i) the energy cost for the Cp–ring slip being vastly overestimated in the gas phase and (ii) the fact that on migratory insertion the prolongation of the Ru–H bond increases the formal positive charge on the ruthenium atom, which is disfavored in the gas phase.

In order to better describe the transition state energy for migratory insertion, several refinements of the model were made. First, the PCM was employed to calculate the transition state in a polar environment utilizing the gas-phase-optimized structure of **TS2** (so-called single-point evaluation of solvent effect). Interestingly, the solvent effect at the gas-phase-optimized geometry reduces the energy of the transition state by 15 kcal/mol ($\epsilon = 9.1$). This is remarkable, when comparing the energy reduction found for the coordination of the imine to **2** (15 kcal/mol versus 7 kcal/mol, respectively) *vide supra*. The second improvement was that the QST-guided search directly within the continuum solvent environment (TS search in the PCM) resulted in a structure with similar geometrical arrangement to that of the gas-phase-optimized **TS2** (Figure 6). However, the energy of the transition state was reduced by 20 kcal/mol. This is consistent with previous single-point evaluation of the transition state energy in the PCM. The high transition state energy of about 20 to 25 kcal/mol for **TS2** does not correlate well to either a reaction proceeding well at low temperatures or the negligible isotope effects found in the stoichiometric hydrogenation of certain imines.^{13,16}

Furthermore, the energy of the TS structure is sensitive to the protonation state of the imine (the structure with the protonated imine has lower energy), which is again the obvious limitation of the solvent-free gas phase calculations. This is illustrated by a more complex transition state structure: bridging water easily mediates the protonation of the Ru-bound amine in **TS2w** (Figure 6). Complex **c** is related to **TS2w** and complex **d** is related to **TS2**. To further optimize the structure, explicit solvent molecules were added to the PCM. To preserve the

(32) Payne, C. K.; Snee, P. T.; Yang, H.; Kotz, K. T.; Schafer, L. L.; Tilley, T. D.; Harris, C. B. *J. Am. Chem. Soc.* **2001**, *123*, 7425.

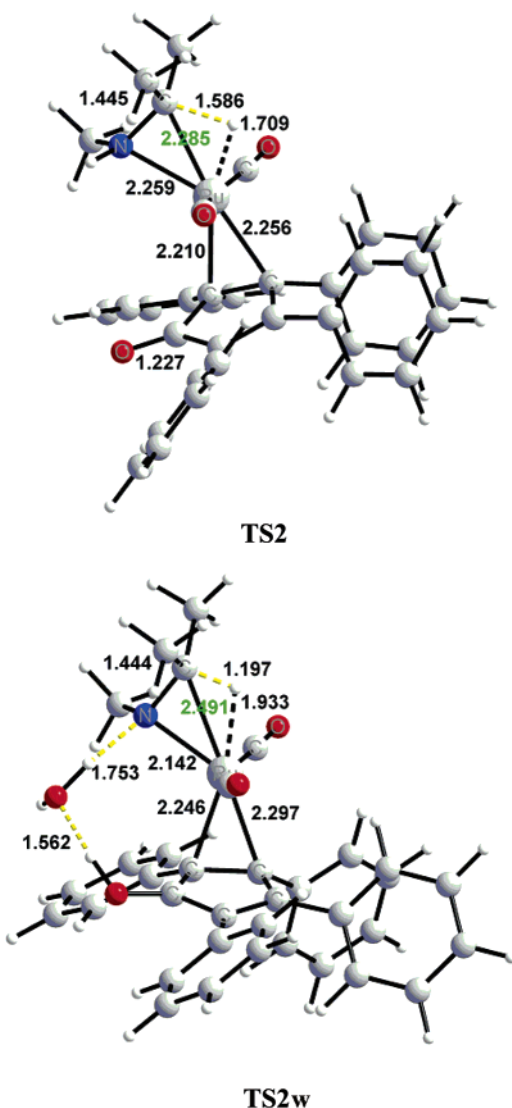


Figure 6. B3LYP/lacvp*-optimized η^2 -TS with the common hydride transfer motif with and without a bridging water molecule. Yellow dashed line indicates the cleaved CH bond, black dashed line indicates a forming RuH bond, and RuC bond distance is shown by a green-colored label. All distances are in Å. QST-guided search method was used.

essential part of the geometry of the transition state, the vicinity of the Ru ion was frozen, while the rest of the system was relaxed. On the basis of the geometry of the gas-phase-optimized TS from Figure 6 we received a final energy of **TS2** of 12 kcal/mol with respect to the initial Ru–imine precursor **a** (identical solvent models with complete geometry optimization were used for **a** and **TS2**, respectively).

Within the accuracy of the method, one can find several well-defined migratory insertion transition state structures that include unsymmetrical η^3 -like bonding of the Ru–Cp ring unit with three different CC bonds of the ring involved. This implies that it is not *one single TS* that limits the rate, but rather that the *reaction has several equivalent reaction pathways* with almost equal height of energy barriers to cross. As a result, the reaction will be 2 or 3 times faster than can be judged by just the activation energy of the single transition state. Even with a relatively high activation energy, the reaction will still be quite efficient due to the combined effect of several equivalent migratory insertion transition states.

The lower activation energy for the migratory insertion (**TS2**) versus coordination (**TS1**) supports experimental data where

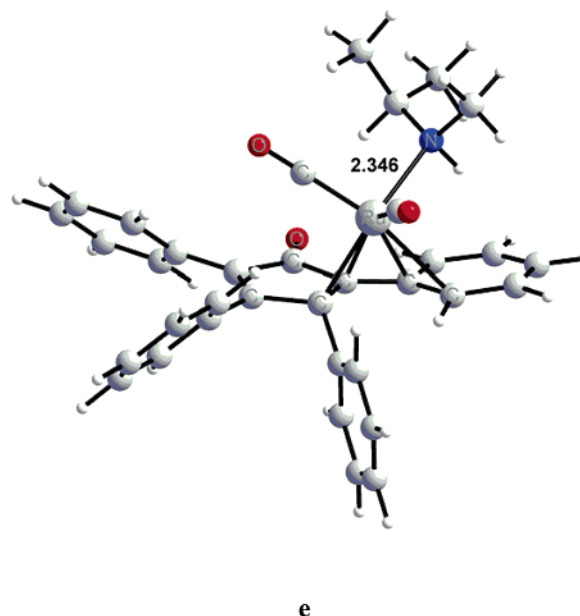


Figure 7. B3LYP/lacvp*-optimized η^2 -like Ru–amine intermediate.

negligible isotope effects were observed in the stoichiometric hydrogenation of electron-rich N-aryl imines by **2**, which clearly shows that the hydrogen transfer is not the rate-determining step.^{13,16} This is in sharp contrast to the kinetic isotope effect of 3.6 found in the hydrogenation of benzaldehyde by **2**.¹⁴ Casey and co-workers have studied the hydrogenation of a very electron-deficient aldimine by **2** and found a kinetic isotope effect close to those found for benzaldehyde.^{16a} This is expected where the weaker basicity of an electron-deficient imine would not promote the crucial proton transfer and induce hydride transfer. As a consequence, the energy of **TS2** would increase and exceed that of **TS1**. More importantly, the kinetic isotope effects found in the reverse transfer dehydrogenation of *N*-phenyl-1-phenylethylamine to the corresponding imine are consistent with a stepwise rate-determining hydride transfer and a fast proton transfer.³³ Thus, the combined isotope effect $k_{\text{CHNH}}/k_{\text{CDND}} = 3.26$ was equal to the individual isotope effect $k_{\text{CHNH}}/k_{\text{CDNH}} = 3.24$, and the other individual isotope effect $k_{\text{NHCD}}/k_{\text{NDCD}}$ was very small, clearly ruling out the concerted hydrogen transfer.^{10b}

Rearrangements in Ru–Amine Complexes: From η^2 to η^4 (TS3**).** If the geometry of **TS2** from Figure 6 is relaxed, a stable (η^2 -cyclopentadienone)ruthenium complex is formed that also involves a η^2 bonding to one of the phenyl groups (**e**, Figure 7). This stable intermediate is 8 kcal/mol higher than the initial Ru–imine precursor **a** in the gas phase and only 5 kcal/mol higher than **a** in the hybrid solvent model or PCM.

We have found that the change in hapticity in ruthenium amine complexes could be well controlled by the transition state such as **TS3** (Figure 8). The energy of this TS is about 10 to 12 kcal/mol in the gas phase and about 9 kcal/mol in the solvent model.

This rearrangement forms the stable η^4 -ruthenium amine complex **b** (Figure 9) and is characterized, first, by the direct coordination of the substrate to ruthenium, and second, by an interaction between NH and CO groups via a weak hydrogen bond, which essentially “locks” the orientation of Ru(CO)₂–amine group on the Cp ring. Contrary to **a**, η^4 -Ru–amine adduct

(33) In the reverse reaction (the dehydrogenation) the β -elimination step precedes the decoordination, and therefore a kinetic isotope effect is expected and is also observed.

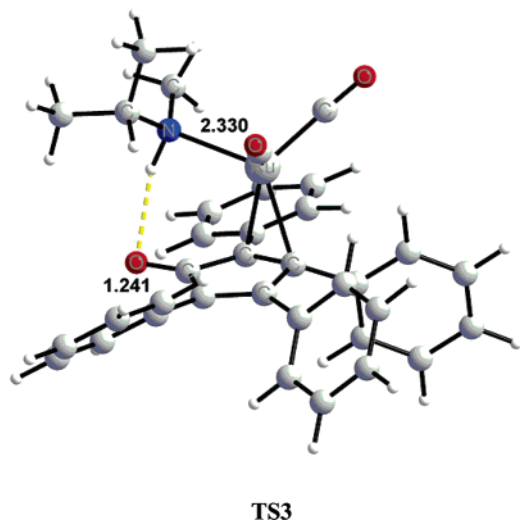


Figure 8. B3LYP/lacvp*-optimized η^2 Ru-amine TS that is responsible for the change in hapticity of Ru-Cp complexes.

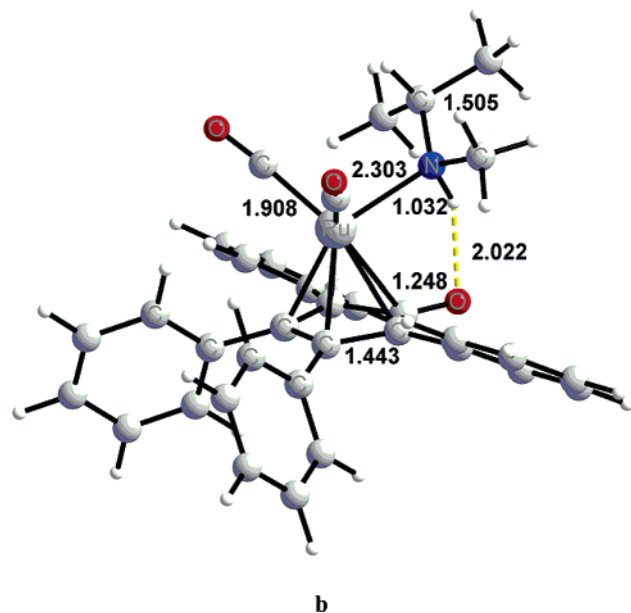


Figure 9. B3LYP/lacvp*-optimized structure of the η^4 -Cp-Ru-amine complex. The longest Ru-C bonds are 2.50 Å (the two Ru-CO bonds), while the other Ru-C distances are 2.3 Å (carbon atoms on the side of the ring) and 2.6 Å (C-C bond opposite the carbonyl) in a symmetrical arrangement.

b does not seem to offer considerable coordination flexibility. The energy difference between the optimized Ru-imine, **a**, and Ru-amine complexes, **b**, is -20 kcal/mol in the gas phase and -16 kcal/mol in dichloromethane solvent (PCM) in favor of the Ru-amine complex **b**.

We have verified our DFT-optimized structure of larger Ru-amine complexes against the X-ray structure that has been reported in ref 13b. Geometry optimization was performed at the B3LYP/lacvp* level. Agreement between the computed structure (Figure 10) and the X-ray structure is good. The Ru atom appears to be formally pentacoordinated with a bidentate (η^4 -Ph₄C₄CO) ligand, two CO, and diamine, respectively. An increase in the size of the basis set resulted in no appreciable improvement of the geometry.

Both complex **e** and **TS3** are important for explaining the results from the isomerization experiments^{9a,16a} and exchange studies.^{13a,16b} The relative energies of **TS2** and **TS3** would explain the isomerization of certain imines bearing β -hydrogens

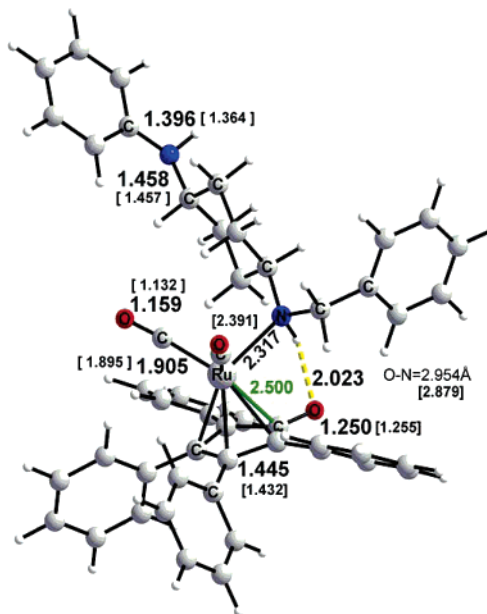


Figure 10. B3LYP/lacvp*-optimized structure of the *trans* isomer of the Ru-amine complex. The corresponding X-ray structure was reported in ref 13b (experimental distances are reported in square brackets). Ru-C1 bond is green, remaining Ru-C distances are 2.312 Å (Ru-C2 and Ru-C5) and 2.255 Å (Ru-C3 and Ru-C4). Experimental data are as follows: Ru-C1 = 2.430 Å; Ru-C2 = 2.250 Å; Ru-C3 = 2.211 Å. The distance between N and the carbonyl carbon atom is 2.954 Å [2.879]. All distances are in Å.

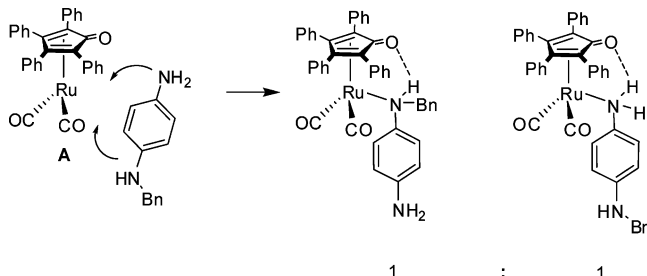
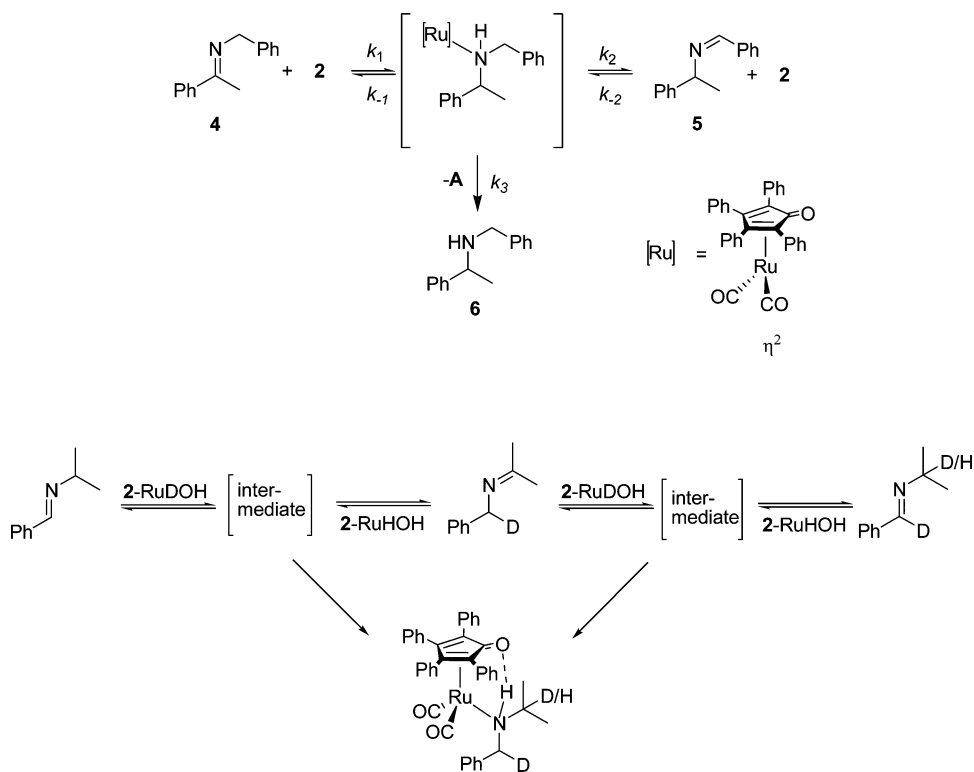


Figure 11. Proposed outer-sphere pathway where the formation of free amine from reduction of p -NH₂-C₆H₄N=CHPh would give a 1:1 mixture of amine complexes.

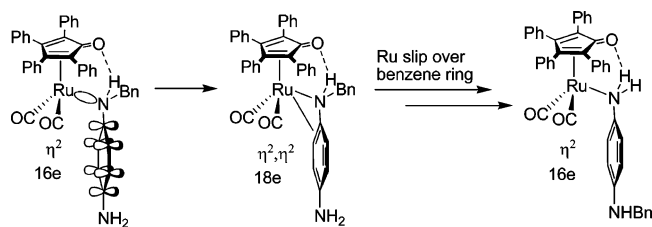
in two different positions (Scheme 4).^{9a,16a} Experimentally, it was found that starting from imine **4** there was a fast isomerization to imine **5**. In light of the computational study this would be explained by **TS3** (k_3) being higher in energy than **TS2** (k_2). Casey and co-workers also found that certain substrates underwent isomerization faster than ruthenium amine complex formation in a stoichiometric hydrogenation by using a deuterium analogue of **2**.¹⁶ They explained the isomerization by an outer-sphere mechanism, where the intermediate indicated in Scheme 4 (lower part) is a cage complex without coordination of nitrogen to ruthenium. The inner-sphere mechanism via coordination of the nitrogen would also explain their results.^{13b}

The outer-sphere concerted mechanism was recently supported by the observation that an imine having an internal trap gave exchange.^{16b} Thus, hydrogenation of p -NH₂-C₆H₄N=CHPh by **2'** gave a 1:1 mixture of [2,5-Ph₂-3,4-Tol₂(η^4 -C₄CO)]-(CO)₂RuNH(CH₂Ph)(C₆H₄- p -NH₂) and [2,5-Ph₂-3,4-Tol₂(η^4 -C₄CO)](CO)₂RuNH₂C₆H₄- p -NHCH₂Ph, which is expected if the free diamine and **A** are formed in an outer-sphere process (Figure 11).

Scheme 4. Isomerization of Imines



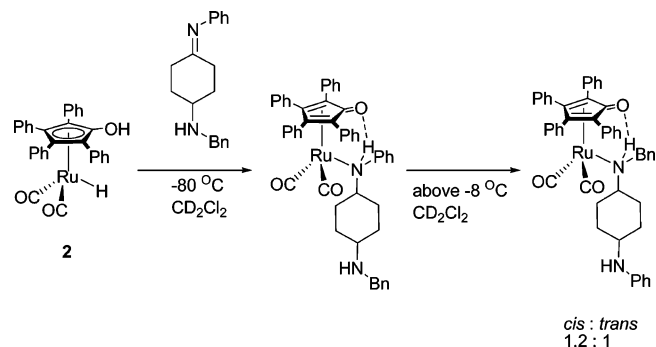
Scheme 5



However, the nitrogens of the diamine in the latter study were connected by an aromatic system, and one cannot exclude the possibility that the internal exchange could occur via the π -system where ruthenium can slip over from one nitrogen to the other in the (η^2 -cyclopentadienone)ruthenium amine intermediate (Scheme 5). This would be explained if **TS3** is close in energy to the ruthenium slipping to the π system of the phenyl ring.³⁴ It is interesting to note that in the (η^2 -cyclopentadienone)-ruthenium intermediate **e** the empty coordination site on ruthenium is filled out by coordination of a double bond in the phenyl substituent of the Cp ring. In the (η^2 -cyclopentadienone)-ruthenium complex in Scheme 5, a coordination of one of the double bonds of the benzene ring of the diamine would lead to a similar stabilization.

The hypothesis that there is an intramolecular exchange at the η^2 stage in the diamine complex (Scheme 5) was recently supported by an experiment where a saturated cyclohexane ring was used instead of a benzene ring as a linker between the nitrogens. In this case only the ruthenium amine complex was formed where the ruthenium binds to the amine originating from the imine.^{13b} Thus, reaction of hydride complex **2** with 4-BnNH-C₆H₉=NPh afforded only [2,3,4,5-Ph₄(η^4 -C₄CO)]Ru(CO)₂NH(Ph)(C₆H₁₀-4-NHBn) at low temperatures and did not rearrange

Scheme 6



until the temperature was raised and the corresponding [2,3,4,5-Ph₄(η^4 -C₄CO)]Ru(CO)₂NH(Bn)(C₆H₁₀-4-NHPh) was observed (Scheme 6).

Summary

To summarize the reaction thermodynamics, the mechanism for the hydrogenation of imines begins with the imine nitrogen binding to the OH of complex **2** (Figure 1). We will designate this hydrogen-bonded intermediate **a** the energy 0 kcal/mol. Coordination of the imine to ruthenium (**TS1**, 15 kcal/mol), in which the ruthenium slips from η^5 to η^3 , gives intermediate **c**. A fast proton transfer is followed by the slower hydride transfer (**TS2** or **TS2w**, 12 kcal/mol), forming η^2 -cyclopentadienone intermediate **e**. Intermediate **e** then rearranges to the final (η^4 -cyclopentadienone)ruthenium amine complex **b** via a transition state that is 9 kcal/mol above **a**. The electronic binding energy of **a** is -12 and -9.6 kcal/mol in the gas phase and PCM, respectively, which will easily compensate for the entropy decrease in the Gibbs free energy, which is normally expected to reduce the binding energy by about 10 kcal/mol. Considering this, the reaction profiles (Figure 12) seem to speak in favor of

(34) Results of computational modeling of the "internal trap" process will be reported elsewhere upon completion.

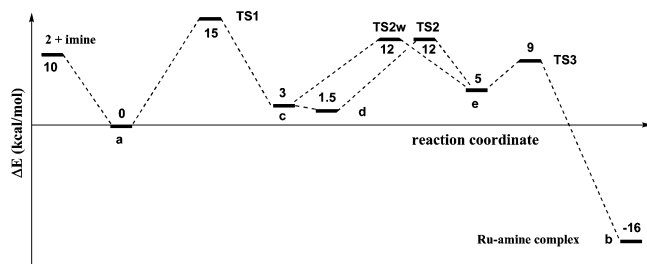


Figure 12. Relative energies of all reaction steps (in kcal/mol), effectively starting with the Ru–imine complex. All energies refer to the “hybrid solvent model” with a few explicit solvent and water molecules combined with the continuum solvent model, PCM. Gas phase and pure PCM data are discussed where appropriate in the text. Electronic binding energy of **a** is -12 and -9.6 kcal/mol in the gas phase and PCM, respectively. Energy difference between **c** and **d** is 1.6 kcal/mol in the gas phase (**c** is lower) and -1.2 kcal/mol in PCM (**d** is lower). All stationary points were calculated with the same basis set (B3LYP/lacvp*, further refined with larger basis; see Computational Details).

a fast reaction that would certainly run even at -70 °C.³⁵ The relative energies of the most important reaction complexes are summarized in Figure 12.

Conclusions

Previous experimental studies on hydrogen transfer with catalyst **1** clearly show the difference between carbonyl compounds/alcohols and imines/amines as substrates. Two mechanisms are currently considered for this type of reaction: an inner-sphere and an outer-sphere mechanism. The outer-sphere pathway^{16b} was previously elucidated by means of DFT methods, while the inner-sphere pathway was left without due attention.

In the present paper we have studied the feasibility of an inner-sphere reaction mechanism. We have developed a robust molecular model that allowed us to characterize the complete reaction pathway including three transition states for the transformation of hydride **2** and imine to ruthenium amine complex **b** where all three may become rate limiting depending on the substrate employed. **TS1** (coordination via ring slippage) and **TS2** (migratory insertion) are quite close in energy, and the difference between them is smaller than the error of the DFT method itself. Importantly, the pathway supported with the calculations in this study is in agreement with experimental data. Furthermore, the mechanism would account for both directions of the reaction coordinate, and this is very important according to the principle of microscopic reversibility.

(35) The rule of thumb is that a reaction runs at room temperature, 298 K, if the activation energy is about 20 to 22 kcal/mol, which corresponds to the barrier of about 15 kcal/mol if the same reaction runs at approximately the same rate at -70 °C.

Technical Details

The calculations of the intermediates were performed as follows. First, geometry optimizations of all intermediate complexes and transition states were carried out using the B3LYP functional³⁶ with the lacvp*/6-31G(d) basis set.^{37,38} All degrees of freedom were optimized, including those of explicit solvent molecules. Transition states were obtained by utilizing QST-guided search and were characterized by the presence of exactly one imaginary vibrational frequency along the appropriate normal mode.

In the second step, B3LYP energies were evaluated for the optimized geometry using a larger triple- ζ basis, lacv3p*/6-311+G(d), with additional diffuse and polarization functions. All computations were performed with the Jaguar v4.0 and v.6.0 suite of *ab initio* quantum chemistry programs.³⁹ Solvent (dichloromethane) was represented with the following parameters: $\epsilon = 9.1$ and probe radius $r_p = 2.33$ Å. Gas-phase-optimized structures were used in the solvation calculations within the self-consistent reaction field model as implemented in the Jaguar computational package.²² Additionally, transition state structures were optimized in the PCM as referenced in the text. All frequency analysis was performed with Jaguar 6.0.

The solvent was modeled using the self-consistent polarized medium²² (SCRF/PCM) with additional solvent molecules and/or water molecules in the second coordination sphere of the complexes studied. Solvent effects related to the coordination of the Ru–Cp unit were double checked by explicit treatment of the coordination sphere in an extended solvent supercluster at the same level of accuracy, B3LYP/lacvp*, and BP86/lacvp as the reported geometry optimizations. The stability of the totally relaxed and optimized explicit solvent environment was ensured by accurate geometry optimization within the PCM, which elevates considerably problems typically associated with solvent–solvent interaction at boundaries of a finite molecular model.

Acknowledgment. This work was supported by grants from the Swedish Research Council. SNAC allocation of computer time at NSC, Linköping, is greatly acknowledged.

Supporting Information Available: Provided are the coordinates and structural parameters of optimized complexes and technical details. This material is available free of charge via the Internet at <http://pubs.acs.org>.

OM070169M

(36) (a) Becke, A. D. *J. Chem. Phys.* **1993**, *98*, 5648. (b) Lee, C.; Yang, W.; Parr, R. G. *Phys. Rev. B* **1988**, *37*, 785.

(37) Hay, P. J.; Wadt, W. R. *J. Chem. Phys.* **1985**, *82*, 299.

(38) (a) Hehre, W. J.; Ditchfield, R.; Pople, J. A. *J. Chem. Phys.* **1972**, *56*, 2257. (b) Francl, M. M.; Pietro, W. J.; Hehre, W. J.; Binkley, J. S.; Gordon, M. S.; Defrees, D. J.; Pople, J. A. *J. Chem. Phys.* **1982**, *77*, 3654. (c) Hariharan, P. C.; Pople, J. A. *Theor. Chim. Acta* **1973**, *28*, 213.

(39) *Jaguar 4.0 and 6.0*; Schrödinger, Inc.: Portland, OR.